



Published in final edited form as:

J Am Coll Cardiol. 2008 November 11; 52(20): 1652–1660. doi:10.1016/j.jacc.2008.06.051.

Ectopic expression of the sodium-iodide symporter enables imaging of transplanted cardiac stem cells *in vivo* by SPECT or PET

John Terrovitis, MD¹, Keng Fai Kwok, BS², Riikka Lautamäki, MD, PhD³, James M Engles, BS³, Andreas S Barth, MD, PhD¹, Eddy Kizana, MBBS, PhD¹, Junichiro Miake, MD, PhD¹, Michelle K Leppo, BS¹, James Fox, BS², Jurgen Seidel, PhD², Martin Pomper, MD, PhD⁴, Richard L Wahl, MD³, Benjamin Tsui, PhD², Frank Bengel, MD³, Eduardo Marbán, MD, PhD¹, and M. Roselle Abraham, MD¹

¹ Cardiology, Johns Hopkins University, Baltimore, MD, USA

² Diagnostic Imaging Physics, Johns Hopkins University, Baltimore, MD, USA

³ Nuclear Medicine, Johns Hopkins University, Baltimore, MD, USA

⁴ Radiology, Johns Hopkins University, Baltimore, MD, USA

Abstract

Objectives—We examined the sodium-iodide symporter (NIS) which promotes *in vivo* cellular uptake of ^{99m}Tc or ¹²⁴I, as a reporter gene for cell tracking by SPECT or PET imaging.

Background—Stem cells offer the promise of cardiac repair. Stem cell labeling is a prerequisite to tracking cell fate *in vivo*.

Methods—The human NIS cDNA was transduced into rat cardiac-derived stem cells (rCDCs) using lentiviral vectors. Rats were injected intra-myocardially with up to 4 million NIS⁺-rCDCs immediately following LAD ligation. Dual isotope SPECT (or PET) imaging was performed, using ^{99m}Tc (or ¹²⁴I) for cell detection and ²⁰¹Tl (or ¹³NH₃) for myocardial delineation. In a subset of animals, high resolution *ex vivo* SPECT scans of explanted hearts were obtained to confirm that *in vivo* signals were derived from the cell injection site.

Results—NIS expression in rCDCs did not affect cell viability and proliferation. NIS activity was verified in isolated transduced cells by measuring ^{99m}Tc uptake. NIS⁺ rCDCs were visualized *in vivo* as regions of ^{99m}Tc or ¹²⁴I uptake within a perfusion deficit in the SPECT and PET images, respectively. Cells could be visualized by SPECT up to day 6 post-injection. *Ex vivo* SPECT confirmed that *in vivo* ^{99m}Tc signals were localized to the cell injection sites.

Corresponding author: M. Roselle Abraham, Department of Medicine, 720 Rutland Ave, Ross 844, Baltimore, MD 21205, (410) 502-2685 / FAX (410) 955-7953, mabraha3@jhmi.edu.

Publisher's Disclaimer: This is a PDF file of an unedited manuscript that has been accepted for publication. As a service to our customers we are providing this early version of the manuscript. The manuscript will undergo copyediting, typesetting, and review of the resulting proof before it is published in its final citable form. Please note that during the production process errors may be discovered which could affect the content, and all legal disclaimers that apply to the journal pertain.

No conflicts of interest to disclose

Conclusion—Ectopic NIS expression allows non invasive *in vivo* stem cell tracking in the myocardium, using either SPECT or PET. The general approach shows significant promise in tracking the fate of transplanted cells participating in cardiac regeneration, given its ability to observe living cells using clinically-applicable imaging modalities.

Keywords

stem cells; imaging; SPECT; PET

Introduction

Stem cells offer the promise of organ repair on demand. Our pre-clinical studies and studies by other groups, in small and large animal models indicate that autologous cardiac-derived stem cells (CDCs) can successfully regenerate myocardium in the setting of ischemic damage (1-4). Despite this initial success, an important problem that remains to be tackled is low levels of transplanted cell survival and engraftment (5-7). *In vivo* stem cell tracking is a pre-requisite to understanding stem cell biology, optimizing engraftment and maximizing the functional benefits of stem cell therapy in the heart(8). The ideal cell-tracking method should be non-toxic, sensitive, specific for the labeled cells and should permit long-term follow-up(9).

Most studies have used direct labeling of stem cells, with agents such as radionuclides or particles prior to transplantation (8, 9). In this study, we adopted a novel approach of using a reporter gene (the sodium-iodide symporter) that is normally expressed in the thyroid, stomach, choroids plexus and salivary gland (10), but not in the heart, to track CDCs after injection into the heart; the sodium-iodide-symporter (NIS) promotes cellular uptake of iodide or pertechnetate (^{99m}Tc) and sodium ions, driven by the transmembrane sodium gradient (11). Remarkably, following ectopic NIS expression, only cells over-expressing NIS will uptake ^{99m}Tc (pertechnetate) or ^{124}I after intravenous injection of these tracers, permitting non-invasive, longitudinal monitoring of stem cell engraftment by SPECT and PET respectively. The main advantage of the reporter gene approach over direct stem cell labeling approaches is that expression of the reporter gene and functional competence of the expressed protein are dependent on cell viability, unlike direct labeling where the label can be taken up by cardiac myocytes or inflammatory cells after labeled cell death, thus confounding quantification of engraftment(12-14).

Methods

Cells

Rat CDCs were cultured from Wistar Kyoto rats as previously described(1, 2) (supplemental methods).

Animal model

WKY rats (n=31) underwent myocardial infarction by permanent ligation of the left anterior descending coronary artery, following which 1-4 million NIS⁺ syngeneic rCDCs were injected intra-myocardially at 2-4 sites (supplemental methods).

Lentivirus preparation

A third-generation lentiviral vector system was used to label the rCDCs(1, 15). Expression of the human NIS gene was driven by constitutively active promoters, CMV (cytomegalovirus promoter) or CAG (composite promoter consisting of the CMV enhancer and chicken beta actin promoter-supplemental methods).

Cell proliferation

A colorimetric proliferation assay was performed to test the effect of ectopic NIS expression on CDC viability/function (supplemental methods).

***In vitro* Angiogenesis Assays** were performed as recommended by the manufacturer (Becton-Dickinson, Franklin Lakes, NJ-supplemental methods).

***In vitro* ^{99m}Tc (pertechnetate) uptake** assay was performed to examine the function of the ectopically expressed NIS (supplemental methods).

PCR. Reverse Transcription (RT)-PCR was performed to confirm NIS-expression in myocardium, 24hrs after injection of NIS-labeled rCDCs (supplemental methods). Quantitative PCR for the rat SRY gene was performed on day 1 and day 8 to confirm CDC engraftment after gender-mismatched rCDC transplantation (supplemental methods).

In vivo imaging

SPECT/CT—Animals were imaged using a Gamma Medica X-SPECT-CT scanner (Gamma Medica, Northridge, CA, USA). SPECT imaging was performed before PET imaging because ¹²⁴I has a relatively long half life (4.2 days) and emits gamma rays that would increase background and decrease contrast during SPECT imaging. The radioisotopes, ^{99m}Tc (7.7±1.7 mCi /285±63MBq) and ²¹⁰Tl (1mCi/37MBq) were injected via the tail vein (n=13; 6 received CMV.NIS cells, 5 CAG.NIS and 2 non-transduced rCDCs), 24hrs after CDC injection. In addition, 3 rats injected with 4×10⁶ CMV.NIS cells were imaged on days 1, 3, 6 and 10 post-transplantation for longitudinal cell-tracking. Images were acquired 1 hour after tracer injection, since this time point has been associated with peak myocardial accumulation of ^{99m}Tc in a previous detailed time course study(16). Dual isotope SPECT was performed to shorten scan time. Details regarding the imaging protocol are provided in the supplemental methods. Resolution of the SPECT system was 1.7mm (Full Width at Half Maximum-FWHM), at the center of the field of view (with a radius of rotation of 5cm and a pinhole aperture of 1mm).

X-ray computed tomography was performed on the same SPECT/CT system (supplemental methods)

PET/CT

¹²⁴I (3.70±1.45mCi/137±54MBq) was injected via the tail vein (n=5; 3 received CAG.NIS CDCs and 2 CMV.NIS CDCs), 24 hours after SPECT imaging and 48 hours after CDC transplantation. A static 30 min acquisition was obtained 1 hour after tracer injection. ¹³NH₃ 1mCi (37MBq) was injected after completion of the iodine acquisition, and was followed by

a 20min static acquisition. Since the ammonia scan was intended only for myocardial delineation and not for quantification of perfusion, the high background from persisting ^{124}I in the blood pool was not of concern, although it could have slightly diminished the contrast between myocardium and LV cavity.

PET images were acquired on a small animal PET system (GE Healthcare Vista). The complete PET imaging protocol is described in the supplemental methods section. Resolution of the system was 1.4mm (FWHM) at the center of the field of view (17). Images after each tracer administration were acquired at exactly the same position.

Co-registration of PET and CT images was performed using rigid body transformation and is described in the supplemental methods section (Supplemental Figure 1).

Ex vivo SPECT imaging

In order to validate the results obtained by *in vivo* imaging and to confirm the origin of the *in vivo* signal, a high resolution *ex vivo* SPECT scan was performed (n=5) after the completion of the *in vivo* experiment (supplemental methods).

Image analysis

All images were analyzed using AMIDE software. (18). A volume of interest (VOI) was drawn to include the bright spot at the cell injection site, for each animal. The same VOI was then placed inside the LV cavity to obtain signal intensities in the blood pool. Contrast Ratio (CR) % was defined as $100 \times [(\text{signal in the cells}) - (\text{signal in blood pool})] / \text{signal in blood pool}$. A detailed description of the signal quantification protocol we employed is provided in the supplemental methods section.

Statistical analysis

Values are reported as mean \pm SD. Repeated measures ANOVA was used for comparison of cell proliferation rates (NIS⁺ vs. non-transduced CDCs) at different time points. The paired t-test was used to compare CR between SPECT and PET images and % uptake of injected dose (%ID) between SPECT images. Statistical analysis was performed using Graph Pad Prism 4 software. A $p < 0.05$ was chosen for statistical significance.

Results

Immunostaining and RT-PCR

Ectopic expression of human NIS in transduced rCDCs was confirmed by immunostaining with a human-specific NIS antibody (Figure 1a). In addition, expression of human NIS mRNA was detected by amplification of a 353bp band using gene specific primers for RT-PCR on mRNA isolated from hearts of animals injected with NIS⁺ rCDCs.

In vitro $^{99\text{m}}\text{Tc}$ (pertechnetate) uptake

Functionally, NIS⁺ cells accumulated $^{99\text{m}}\text{Tc}$ (pertechnetate), an effect that was inhibited by the specific NIS blocker, sodium perchlorate (uptake: $6.0 \pm 0.9\%$ vs. 0.07 ± 0.05 , without and with blocker respectively, Figure 1c); non-transduced cells did not demonstrate any $^{99\text{m}}\text{Tc}$

uptake. We attribute the low in vitro uptake of ^{99m}Tc to rapid tracer efflux from the transduced cells(19, 20). We believe that this property would be favorable for the use of NIS as a reporter gene, since the transient intracellular presence of the radiotracer would reduce the risk of radiotoxicity to the stem cells (20).

Cell viability and function

Over-expression of hNIS did not significantly affect rCDC viability or proliferation, when compared to non-transduced control cells ($p=0.718$ by repeated measures ANOVA; Figure 2a). Likewise, cells over-expressing hNIS did not demonstrate any decrease in their cardiogenic potential (determined by additional transduction of cells with a lentiviral construct expressing firefly luciferase under transcriptional control of a cardiac-specific promoter (NCX1 or cardiac sodium-calcium exchanger); Figure 2b) (21) or in their angiogenic capacity (determined by their ability to form vascular tubes in an angiogenesis assay; Figure 2c-e).

In vivo SPECT

^{201}Tl perfusion scans lead to adequate visualization of the viable myocardium in all experiments. A large perfusion deficit due to infarction was seen in the middle and apical segments of the anterior and anterolateral walls and septum. Cells expressing hNIS were identified as a region of increased tracer uptake within the perfusion deficit area, (Figure 3a-c) in all animals on day 1 post-transplantation (11/11, 2 injected with 10^6 cells and 9 with 2×10^6), whereas, in animals that received control, non-transduced CDCs, ($n=2$, one injected with 10^6 cells and one with 2×10^6), the only cardiac ^{99m}Tc (pertechnetate) signal was derived from the blood pool (Figure 4a-c). ^{99m}Tc (pertechnetate) uptake of the hNIS cells (% of Injected Dose-ID-) was 0.08 ± 0.07 ($n=11$); animals injected with CMV-NIS transduced cells had a significantly higher pertechnetate uptake than animals injected with CAG-NIS transduced cells ($0.12 \pm 0.07\%$ vs. $0.03 \pm 0.03\%$, $p=0.027$), in concordance with our in vitro data comparing the two promoters, using firefly luciferase as the reporter gene (Supplemental Methods and Supplemental Figure 2). Contrast Ratio (CR) was also higher when CDCs transduced with CMV-NIS were used ($70 \pm 40\%$ with CMV-NIS cells vs. $28 \pm 29\%$ for CAG-NIS cells $p=0.085$), indicating higher expression levels of NIS in CMV-NIS cells and consequently higher pertechnetate uptake. These results underscore the importance of the promoter and consequently transgene expression levels on the outcome of in vivo imaging. Importantly, CR between injection site and myocardium and lung was high ($115 \pm 49\%$ and $202 \pm 121\%$, respectively), indicating lack of specific uptake of pertechnetate by tissues that do not normally express NIS. In fact, CR between the region of the myocardium containing the perfusion deficit (corresponding to the injection site) and the LV cavity was $-18 \pm 10\%$ in the animals injected with non-transduced cells; this indicates a brighter signal in the blood pool than in the hypoperfused infarcted myocardium.

In animals ($n=3$) injected with 4×10^6 CDCs that underwent serial SPECT imaging, CDCs were identified on day 1, 3 and 6 post-injection (CR was 452 ± 29 , 196 ± 71 and $131 \pm 66\%$, on day 1, 3 and 6 respectively-Figure 7), but not on day 10, where the CR was $1.1 \pm 14\%$, between the area of brightest signal in the myocardium and the LV cavity. These results indicate that NIS can be used for longitudinal stem cell tracking after transplantation.

***In vivo* PET**

$^{13}\text{NH}_3$ perfusion scans generated clear images of the viable myocardium in 5/5 animals that underwent small animal PET. All animals received 2×10^6 cells (2 received CAG.NIS and 3 CMV.NIS cells). Injection sites were identified in 3/5 animals (2 had received CMV.NIS and one CAG.NIS cells) (Figure 5d-f, Figure 6a-c). CR obtained by PET was low ($18 \pm 8\%$) in this particular experimental setting (dedicated small animal scanner and ^{124}I as tracer), suggesting limitations of ^{124}I as a positron emitting tracer. Co-registration of the PET images with CT confirmed signal localization in myocardium (Figure 6).

***Ex vivo* SPECT**

An ex vivo cardiac SPECT scan was performed in 5 animals after the completion of in vivo imaging in order to verify that signal was indeed from cells and not from the blood pool. A region of increased $^{99\text{m}}\text{Tc}$ (pertechnetate) uptake that was similar in appearance to the in vivo signal was identified within the myocardium, but the CR was considerably higher ($323 \pm 293\%$ vs $70 \pm 40\%$), due to lack of signal from the blood pool (Supplemental Figure 3).

Real Time PCR

Quantitative PCR confirmed that rapid cell loss occurred within the first week after intra-myocardial CDC implantation. We found that $13.2 \pm 3.6\%$ of the injected cells were retained on day 1, and $2.8 \pm 1.8\%$ on day 8 after transplantation (Figure 8). Based on these PCR results, we estimate that the threshold for CDC detection by SPECT is approximately 150,000 cells.

Discussion

Tracking stem cell fate after transplantation is essential for elucidation of the mechanisms underlying stem cell engraftment and resultant functional benefit. This is the first report using human NIS as the reporter gene to track stem cells in the heart by SPECT and PET imaging. The advantages of this approach are that it is translatable into the clinical setting because it employs a transgene that is non-immunogenic and the radiotracer $^{99\text{m}}\text{Tc}$ with SPET scanning, both of which are widely available and FDA-approved.

To date, most cell tracking studies have used *in vitro* cell labeling with iron nanoparticles followed by in vivo MRI (22-24). Despite the significant advantages of MRI (high sensitivity, excellent anatomical and functional data), we and others recently showed that iron-derived signals can persist in the myocardium and can be detected by MRI long after cells have been destroyed, generating false-positive signals (12-14). Genetic labeling, on the other hand, offers the important advantage that only cells expressing the transgene will generate signal (25, 26).

Further significance of the present study lies in its potential for clinical translation. Pertechnetate SPECT is a widely available, clinically approved, relatively low cost, imaging modality. Results obtained by SPECT imaging in small animals can be easily tested in larger animal models or humans, using clinical SPECT systems. Importantly, there has been substantial progress in absolute signal quantification in clinical SPECT systems in recent

years, a fact that strengthens even further the role of SPECT for *in vivo* stem cell tracking(27).

The wild type or mutated herpes virus thymidine kinase gene is another transgene that has been successfully used for stem cell tracking by SPECT or PET imaging. hNIS has two important advantages over herpes virus thymidine kinase: it utilizes widely available tracers, therefore no specialized radio-synthesis facilities are needed and it is a human gene, precluding an immune response if applied clinically.

To date, only direct labeling of stem cells by ^{111}In -oxine or $^{99\text{m}}\text{Tc}$ Hexamethylpropylenamine Oxime (Tc-HMPAO) has been used for stem cell tracking by SPECT (28, 29). These techniques only permit stem cell tracking over a short period of time, determined by the tracer half lives (2.8days for indium and 5.8hrs for $^{99\text{m}}\text{Tc}$) and also pose the risk of radiotoxicity to the cells. In the present study, we showed that human NIS expression in cardiac-derived stem cells is non-toxic and can promote adequate tracer uptake to allow *in vivo* cell imaging. Even in short term studies, visualizing cells using a reporter gene approach is superior to any direct labeling method, since signal in the former is always derived from viable transplanted cells (high specificity). With direct labeling, a fraction of the signal might be derived from tracer released by dead cells and persisting at the injection site (in the extracellular space or uptaken by other cell types), generating false positives and undermining the biological interpretation of the *in vivo* imaging studies.

Despite the widespread availability of SPECT, PET is attractive for stem cell studies because it is more sensitive and the signal is readily quantifiable. Here, we showed the feasibility of tracking CDCs in the myocardium by ^{124}I PET, using hNIS as reporter gene. However, the contrast achieved was sub-optimal, when compared to our SPECT results. Possible explanations for this unexpected finding include a) ^{124}I is not a pure positron emitter; only 25.6% of the activity is emitted as positrons, resulting in significantly lower efficiency for this agent as a PET tracer, b) the emission of coincident, high energy, gamma rays significantly increases scatter and background activity, leading to considerable image deterioration and c) positrons emitted by ^{124}I annihilate at a relatively long distance (approximately 1.4mm in comparison to 0.2mm for positrons emitted by ^{18}F) in relation to their site of production, leading to degradation of spatial resolution(30). This adverse characteristic is of greater importance in small animal studies, where small errors in localization are large in relation to the size of the myocardium. Despite the disadvantages, there is potential for improvement: the positron emitter $^{94\text{m}}\text{Tc}$ -pertechnetate can be used instead of ^{124}I for clinical translation; although $^{94\text{m}}\text{Tc}$ is not a pure positron emitter, it has a more attractive half life (52.5min instead of 4.2 days for ^{124}I) and does not affect thyroid gland function.

Several limitations have to be acknowledged. The present proof-of-concept study was confined to assessment of CDC engraftment, not functional effects of transplantation, in a small animal model; feasibility in a large animal model needs to be demonstrated before definitive conclusions about clinical translatability can be drawn. However, application in larger animals is expected to be less challenging, since a considerably higher number of cells will be injected, resulting in higher tracer uptake and stronger *in vivo* signals.

Another fact that limits immediate translation of our results into patients is the use of lentivirus vectors that have not yet been approved for human use due to safety concerns. This is not an inherent feature of the method; routine plasmid transfection followed by cytotoxic selection could equally well be used to establish NIS-expressing cell lines.

In conclusion, this is the first report of *in vivo* cardiac-derived stem cell tracking by SPECT and PET, using the sodium iodide symporter as the reporter gene. This technique is readily translatable into the clinical realm and could be expected to improve our understanding of *in vivo* stem cell biology and eventually the functional effects of stem cell transplantation in the heart.

Supplementary Material

Refer to Web version on PubMed Central for supplementary material.

Acknowledgments

The work was supported by the Donald W. Reynolds Foundation, the NHLBI and the WW Smith Foundation (MRA). ASB was supported by a grant from the German Research Foundation (DFG, grant BA 3341/1-1).

Abbreviations

SPECT	Single Photon Emission Computed Tomography
PET	Positron Emission Tomography
CT	Computed Tomography
MRI	Magnetic Resonance Imaging

References

1. Messina E, De AL, Frati G, et al. Isolation and expansion of adult cardiac stem cells from human and murine heart. *Circ Res*. 2004; 95:911–21. [PubMed: 15472116]
2. Smith RR, Barile L, Cho HC, et al. Regenerative potential of cardiosphere-derived cells expanded from percutaneous endomyocardial biopsy specimens. *Circulation*. 2007; 115:896–908. [PubMed: 17283259]
3. Dawn B, Stein AB, Urbanek K, et al. Cardiac stem cells delivered intravascularly traverse the vessel barrier, regenerate infarcted myocardium, and improve cardiac function. *Proc Natl Acad Sci U S A*. 2005; 102:3766–71. [PubMed: 15734798]
4. Linke A, Muller P, Nurzynska D, et al. Stem cells in the dog heart are self-renewing, clonogenic, and multipotent and regenerate infarcted myocardium, improving cardiac function. *Proc Natl Acad Sci U S A*. 2005; 102:8966–71. [PubMed: 15951423]
5. Suzuki K, Murtuza B, Beauchamp JR, et al. Role of interleukin-1beta in acute inflammation and graft death after cell transplantation to the heart. *Circulation*. 2004; 110:II219–II224. [PubMed: 15364866]
6. Suzuki K, Murtuza B, Beauchamp JR, et al. Dynamics and mediators of acute graft attrition after myoblast transplantation to the heart. *FASEB J*. 2004; 18:1153–5. [PubMed: 15155562]
7. Yau TM, Kim C, Ng D, et al. Increasing transplanted cell survival with cell-based angiogenic gene therapy. *Ann Thorac Surg*. 2005; 80:1779–86. [PubMed: 16242455]
8. Frangioni JV, Hajjar RJ. In vivo tracking of stem cells for clinical trials in cardiovascular disease. *Circulation*. 2004; 110:3378–83. [PubMed: 15557385]

9. Bengel FM, Schachinger V, Dimmeler S. Cell-based therapies and imaging in cardiology. *Eur J Nucl Med Mol Imaging*. 2005; 32(Suppl 2):S404–S416. [PubMed: 16205898]
10. Dohan O, De V, Paroder V, et al. The sodium/iodide Symporter (NIS): characterization, regulation, and medical significance. *Endocr Rev*. 2003; 24:48–77. 1. [PubMed: 12588808]
11. Zuckier LS, Dohan O, Li Y, Chang CJ, Carrasco N, Dadachova E. Kinetics of perrhenate uptake and comparative biodistribution of perrhenate, pertechnetate, and iodide by NaI symporter-expressing tissues in vivo. *J Nucl Med*. 2004; 45:500–7. [PubMed: 15001694]
12. Higuchi T, Anton M, Seidl S, Bengel FM, Bortnar R, Schwaiger M. Multimodality Monitoring of Cardiac Cell Therapy by PET and MRI. *Circulation*. 2007; 116 abstr.
13. Amsalem Y, Mardor Y, Feinberg MS, et al. Iron-oxide labeling and outcome of transplanted mesenchymal stem cells in the infarcted myocardium. *Circulation*. 2007; 116:138–145. [PubMed: 17846324]
14. Terrovitis J, Stuber M, Youssef A, et al. Magnetic resonance imaging overestimates ferumoxide-labeled stem cell survival after transplantation in the heart. *Circulation*. 2008; 117:1555–62. [PubMed: 18332264]
15. Zufferey R. Production of lentiviral vectors. *Curr Top Microbiol Immunol*. 2002; 261:107–21. [PubMed: 11892243]
16. Miyagawa M, Beyer M, Wagner B, et al. Cardiac reporter gene imaging using the human sodium/iodide symporter gene. *Cardiovasc Res*. 2005; 65:195–202. [PubMed: 15621047]
17. Wang Y, Seidel J, Tsui BM, Vaquero JJ, Pomper MG. Performance evaluation of the GE healthcare eXplore VISTA dual-ring small-animal PET scanner. *J Nucl Med*. 2006; 47:1891–900. [PubMed: 17079824]
18. Loening AM, Gambhir SS. AMIDE: a free software tool for multimodality medical image analysis. *Mol Imaging*. 2003; 2:131–7. [PubMed: 14649056]
19. Haberkorn U, Henze M, Altmann A, et al. Transfer of the human NaI symporter gene enhances iodide uptake in hepatoma cells. *J Nucl Med*. 2001; 42:317–25. [PubMed: 11216532]
20. Haberkorn U, Kinscherf R, Kissel M, et al. Enhanced iodide transport after transfer of the human sodium iodide symporter gene is associated with lack of retention and low absorbed dose. *Gene Ther*. 2003; 10:774–80. [PubMed: 12704416]
21. Barth AS, Kizana E, Smith RR, et al. Lentiviral vectors bearing the cardiac promoter of the na(+)-ca(2+) exchanger report cardiogenic differentiation in stem cells. *Mol Ther*. 2008; 16:957–64. [PubMed: 18388932]
22. Frank JA, Miller BR, Arbab AS, et al. Clinically applicable labeling of mammalian and stem cells by combining superparamagnetic iron oxides and transfection agents. *Radiology*. 2003; 228:480–7. [PubMed: 12819345]
23. Hill JM, Dick AJ, Raman VK, et al. Serial cardiac magnetic resonance imaging of injected mesenchymal stem cells. *Circulation*. 2003; 108:1009–14. [PubMed: 12912822]
24. Kraitchman DL, Heldman AW, Atalar E, et al. In vivo magnetic resonance imaging of mesenchymal stem cells in myocardial infarction. *Circulation*. 2003; 107:2290–3. [PubMed: 12732608]
25. Herschman HR. Noninvasive imaging of reporter gene expression in living subjects. *Adv Cancer Res*. 2004; 92:29–80. [PubMed: 15530556]
26. Massoud TF, Gambhir SS. Molecular imaging in living subjects: seeing fundamental biological processes in a new light. *Genes Dev*. 2003; 17:545–80. [PubMed: 12629038]
27. Stodilka RZ, Blackwood KJ, Kong H, Prato FS. A method for quantitative cell tracking using SPECT for the evaluation of myocardial stem cell therapy. *Nucl Med Commun*. 2006; 27:807–13. [PubMed: 16969264]
28. Goussetis E, Manginas A, Koutelou M, et al. Intracoronary infusion of CD133+ and CD133-CD34+ selected autologous bone marrow progenitor cells in patients with chronic ischemic cardiomyopathy: cell isolation, adherence to the infarcted area, and body distribution. *Stem Cells*. 2006; 24:2279–83. [PubMed: 16794269]
29. Kraitchman DL, Tatsumi M, Gilson WD, et al. Dynamic imaging of allogeneic mesenchymal stem cells trafficking to myocardial infarction. *Circulation*. 2005; 112:1451–61. [PubMed: 16129797]

30. Yao R, Balakrishnan S, Ambwani S, Rathod V, Yiping S. Quantitative iodine-124 imaging on animal PET. 2005 IEEE Nuclear Science Symposium Conference Record. 2007; 3:1649–1652.

Author Manuscript

Author Manuscript

Author Manuscript

Author Manuscript

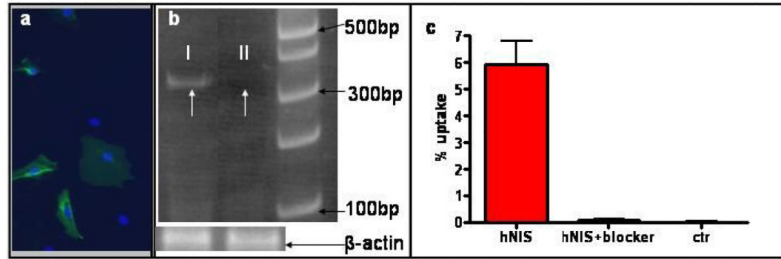


Figure 1. Confirmation of hNIS-expression

(a) Immunostaining confirmed the expression of hNIS (green) in rCDCs after lentiviral transduction (nuclei were counterstained by blue Hoechst dye). (b) Human NIS mRNA was detected by RT-PCR in rat hearts after transplantation of NIS⁺ rCDC (band at 353bps; white arrow I). White arrow for II indicates the lack of a specific band in a rat heart injected with the same number of NIS⁻ cells. (c) Confirmation of hNIS activity in transduced cells. NIS transduction promoted *in vitro* ^{99m}Tc (pertechnetate) uptake by NIS⁺ rCDCs; this uptake was abolished by the specific NIS blocker sodium perchlorate (100μM), (two independent experiments, each condition tested in triplicate).

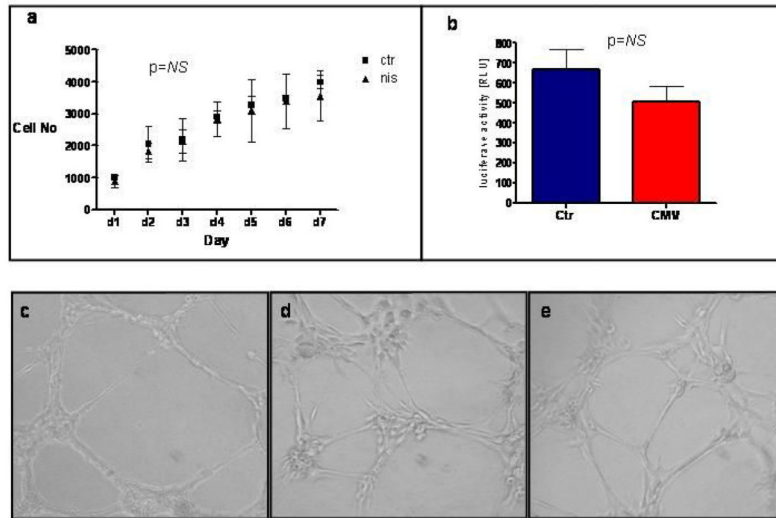


Figure 2. Effect of hNIS over-expression on cell viability, proliferation and function
 (a) There was no difference in viability and proliferation of NIS⁺ vs. non-transduced rCDCs.
 (b) Additional transduction with a lentiviral construct expressing firefly luciferase under the transcriptional control of a cardiac-specific promoter (NCX1, cardiac sodium-calcium exchanger) indicated no decrease in the cardiogenic potential of hNIS expressing cells compared to controls. (c-e) Angiogenesis and vascular tube formation assays. Representative images of Human Vascular Endothelial Cells as positive controls (c), non-transduced rCDCs (d), and rCDCs transduced with hNIS (e). The ability to form vascular structures was preserved after transduction with hNIS.

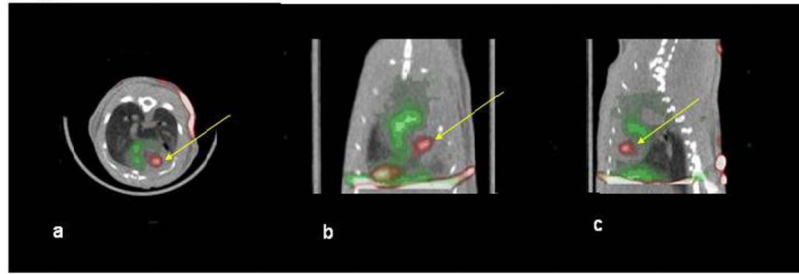


Figure 3. Dual isotope SPECT/CT of an animal injected with hNIS expressing cells
Red: ^{99m}Tc uptake, Green: ^{201}Tl uptake. There is a clear intra-myocardial region (yellow arrow) corresponding to the rCDC injection site within a perfusion deficit. Non-infarcted myocardium appears green due to ^{201}Tl uptake. The liver was also visualized due to uptake of ^{201}Tl . a: transverse, b: coronal, c: sagittal slice orientation.

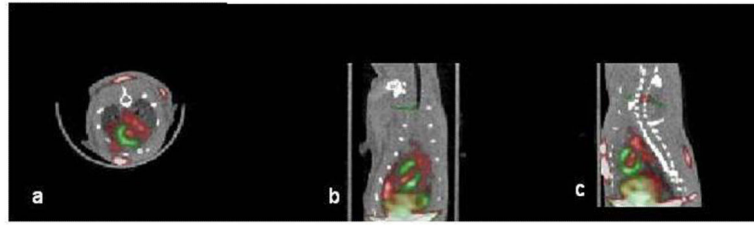


Figure 4. Dual isotope SPECT/CT of an animal injected with non-transduced cells
Red: ^{99m}Tc uptake, Green: ^{201}Tl uptake. The only Tc signal in the cardiac region is derived from the blood pool (atrial and ventricular cavities). a: transverse, b: coronal, c: sagittal slice orientation.

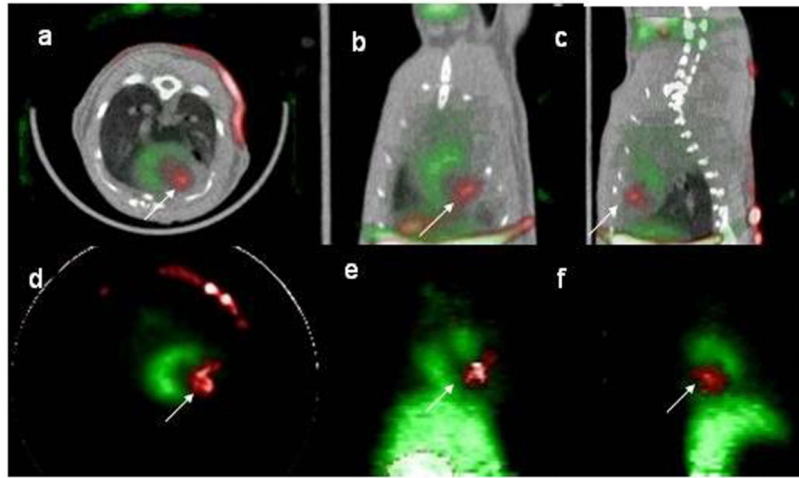


Figure 5. SPECT and PET imaging of an animal injected with hNIS expressing cells
a-c: SPECT/CT 24hrs after cell injection, Red: ^{99m}Tc uptake, Green: ^{201}Tl uptake. White arrow points signal from hNIS expressing rCDCs. a: transverse, b: coronal, c: sagittal slice orientation. d-f: PET of the same animal, at 48hrs after cell injection. Red: ^{124}I uptake, Green: $^{13}\text{NH}_3$ uptake. White arrow points at signal from hNIS expressing cells. d: transverse, e: coronal, f: sagittal slice orientation.

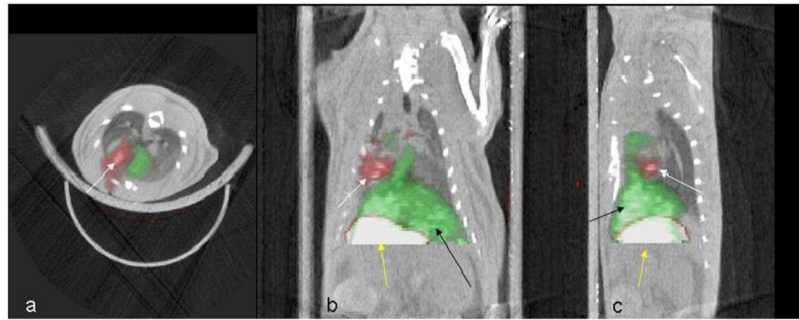


Figure 6. Successful PET/CT co-registration based on the 18 fluoride PET images
Red: ^{124}I uptake. White arrow points to signal from hNIS expressing rCDCs. The stomach takes up ^{124}I and is visualized in the image (yellow arrow). Non-infarcted myocardium and liver (black arrow) take up $^{13}\text{NH}_3$ and appear green in the perfusion scan. a: transverse, b: coronal, c: sagittal slice orientation.

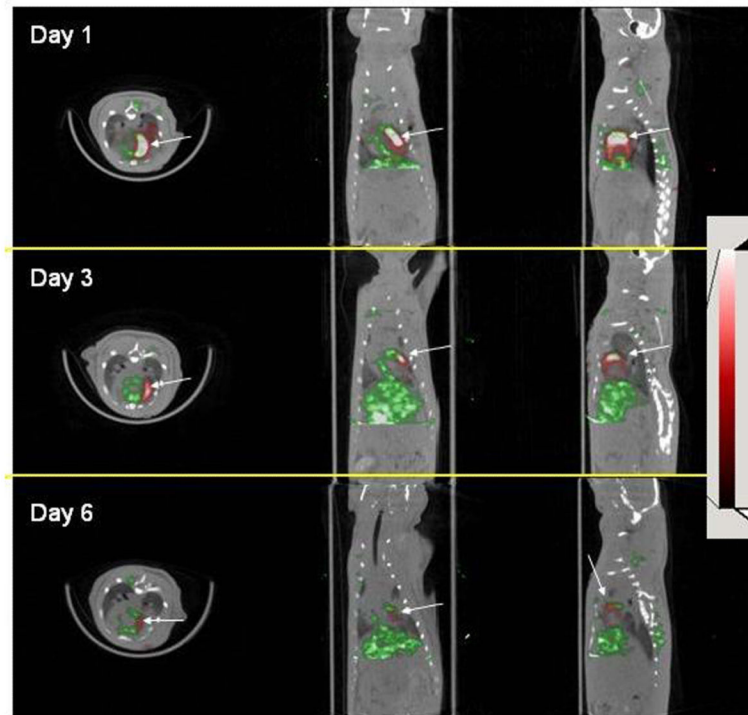


Figure 7. Longitudinal tracking of hNIS expressing cell by SPECT

A. Day 1 after cell injection, B: day 3 after cell injection, C: day 6 after cell injection. Arrows point to signal from engrafted cells. Display settings are identical in all images.

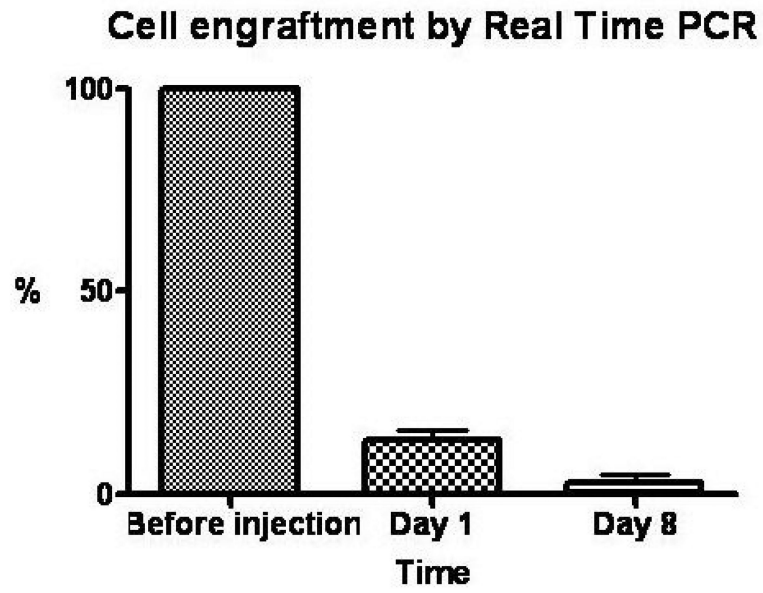


Figure 8. CDC engraftment by quantitative PCR

Column histogram reveals percentage cell engraftment on days 1 and 8 relative to baseline.

Rapid cell loss occurs within 8 days after intramyocardial cell delivery.